An Essential Role for the C-Terminal Domain of A Dragline Spider Silk Protein in Directing Fiber Formation

Shmulik Ittah,[†] Shulamit Cohen,[†] Shai Garty,[‡] Daniel Cohn,[‡] and Uri Gat*[,†]

Department of Cell and Animal Biology, Silberman Life Sciences Institute and Casali Institute of Applied Chemistry, Edmond Safra Campus at Givat-Ram, The Hebrew University, Jerusalem 91904, Israel

Received February 8, 2006; Revised Manuscript Received March 29, 2006

We have employed baculovirus-mediated expression of the recombinant *A. diadematus* spider dragline silk fibroin *rADF*-4 to explore the role of the evolutionary conserved C-terminal domain in self-assembly of the protein into fiber. In this unique system, polymerization of monomers occurs in the cytoplasm of living cells, giving rise to superfibers, which resemble some properties of the native dragline fibers that are synthesized by the spider using mechanical spinning. While the C-terminal containing rADF-4 self-assembled to create intricate fibers in the host insect cells, a C-terminal deleted form of the protein (rADF-4-ΔC) self-assembled to create aggregates, which preserved the chemical stability of dragline fibers, yet lacked their shape. Interestingly, ultrastructural analysis showed that the rADF-4-ΔC monomers did form rudimentary nanofibers, but these were short and crude as compared to those of rADF-4, thus not supporting formation of the highly compact and oriented "superfiber" typical to the rADF-4 form. In addition, using thermal analysis, we show evidence that the rADF-4 fibers but not the rADF-4-ΔC aggregates contain crystalline domains, further establishing the former as a veritable model of authentic dragline fibers. Thus, we conclude that the conserved C-terminal domain of dragline silk is important for the correct structure of the basic nanofibers, which assemble in an oriented fashion to form the final intricate natural-like dragline silk fiber.

Introduction

Spiders can synthesize several types of silk fibers that are the products of specialized abdominal glands, which include the major ampullate gland that secretes the silk proteins (spidroins) constituting the extremely tough dragline fiber utilized for the web frame, radii, and the lifeline thread of the spider.[1−3] The ampullate glands secrete two proteins termed spidroin 1 (MaSp1) and spidroin 2 (MaSp2), which are the main components of the final silk fiber that is drawn by the spider.[4−7] Study of the spider silk protein components and of their encoding genes has shown that the ampullate spidroins such as other fiber-forming structural fibroins have high molecular weights (estimated at 200−350 kDa), of which a large part consists of multiple repetitive sequences.[2,8,9] In the ampullate spidroins, the multiple repeats contain polyalanine stretches, which are thought to form crystalline regions conferring strength to the fiber, interspersed with glycine-rich regions of various conformations that are speculated to provide the elasticity of the fiber.[1,2,10−12] While there is substantial evidence that the central repeats define the mechanical properties of the different fibroins, it is still unclear what is the role (if any) of the flanking nonrepetitive N- and C-termini in fiber formation. Due to the length of the spidroins' mRNAs and to their repetitive nature, it was difficult to obtain N-termini sequence data, which was only available for the flagelliform (spiral capture silk) spidroins; analysis indicated that like in other fibroins this domain is hydrophilic and may assume a globular structure.[13] Very recently, sequences of genomic clones obtained from several species allowed the derivation of several dragline N-terminal coding regions and demonstrated that this region is the most highly conserved in the entire coding region.[14]

When multiple spidroin C-terminal sequences were compared, it was found that this particular domain is highly conserved between major ampullate proteins from different species (75% identity) and also closely related to C-termini of minor ampullate spidroins.[5,13,15] A recent study by the Weisshart group demonstrated that indeed the C-terminal domains of *N. clavipes* dragline spidroins are part of the spinning dope of the gland as well as present in the final fiber,[16] and it has been suggested that the conserved cysteine in these domains may elicit dimer formation of possible importance for the fiber's mechanical qualities.[5,16] Further studies from this group used bacterially expressed recombinant fusion peptides representing repetitive C-terminal spidroin sequences and their combinations, which were adsorbed to glimmer surfaces, followed by observation of the structures that were formed by atomic force microscopy. These experiments indicated that forms of MaSp peptides containing repetitive only or repetitive plus C-terminal parts both tend to form aggregates, which resemble protofilaments of about the same length. However, the addition of the C-terminus enhanced the lateral growth of these aggregates as compared to the repetitive domain-only peptides.[17] Thus, the authors suggest that the C-terminal domains play a structural role in fiber spinning in that they may allow high solubility or precipitation out of solution according to the environmental conditions along the spider gland tract and that the conserved cysteine residue in them may be important for their polymerization-inducing function.[17]

In this study, we further explore the structure of the fibers produced by self-assembly of dragline silk proteins expressed in insect cells[18] and directly examine the role of the C-termini in their polymerization. Our results clearly demonstrate that the C-terminal domain of ADF-4 is necessary for the proper

* Address correspondence to Uri Gat: Tel/fax 972 2 6585920; e-mail gatu@vms.huji.ac.il.

[†] Department of Cell and Animal Biology.

[‡] Casali Institute of Applied Chemistry.

10.1021/bm060120k CCC: $33.50
Published on Web 05/13/2006

structure of the basic fibrils as well as for the oriented assembly of the rADF-4 superfiber, a process that occurs in the cytoplasm of live cells and does not rely on disulfide bond formation. Although this system of polymerization is different than the natural mechanical drawing performed by the spider, much could still be in common, as the resulting structures share similarities in shape and in chemical resistance.[18]

Materials and Methods

Donor Plasmids Construction. Construction of the basic donor plasmid, pFastBacHTa, containing partial cDNAs of *ADF*-4 (genebank entry U47856) has been previously described.[18] Two variants of this donor plasmid were constructed, an HA-tagged version, replacing the original His_6-tag, and a C-terminal-deleted form (*rADF*-4-ΔC).

Replacing the N-terminal His_6-tag by the HA-tag took place by PCR using a sense primer coding for the HA-tag (underlined), preceded by an *Rsr II* restriction site (bold) located upstream to the initiating ATG (italic) and an anti-sense primer containing a 3′ *Spe I* restriction site located 111 bases downstream of the initiating ATG. Sense primer is (5′-AAAACT**CGGTCCG**AAACC*ATG*TCGTACCCATACGATGTG-CCAGATTACGCCGATTACGATATCCCAACGACC-3′). Anti-sense primer is (5′-TCCACTAGTTGAGCTCGTCGACG-3′). The pFastBacHTa-ADF-4 plasmid and the PCR product were digested using *Rsr II* and *Spe I*, purified, and ligated.

Deletion of the C-terminal domain (112 amino acids) took place using PCR with the following primers: A sense primer containing an *Eco0109* restriction site (underlined), which in the *ADF*-4 coding sequence is located between the repetitive and C-terminal coding regions, followed by the ORF's stop codon (bold) and its 18 downstream bases. An anti-sense primer coding for a 3′ *Hind III* restriction site located 150 bases downstream of the above stop codon. Sense primer is (5′-GATCAAGGCCCT**TAA**ACACTTGGTAAAA-TATAG-3′). Anti-sense primer is (5′-TCGACAAGCTTGGTACCGCA-3′).

The pFastBacHTa-*ADF*-4 vector and the PCR product were excised with *Eco0109* and *Hind III*, purified, and ligated, thus removing the C-terminus and introducing a stop codon at the end of the repetitive zone.

Cell Culture, Production of Recombinant Baculovirus, and Expression of Dragline Silk Proteins. These were performed as previously described.[18]

Purification of rADF-4 Fibers and ΔC Aggregates. Infected cells were harvested 3−5 days postinfection and centrifuged for 10 min at 16 000 g. The cell pellets was resuspended in a 10% SDS solution and boiled for 1 h, and protein assemblies were sedimented as above. Typical yields of purified fibers/aggregates were about 50 mg/L of Sf9 insect cell culture. Purified fibers/complexes were resuspended at desired solution and volume.

Immunocytochemistry. Cells grown on cover slips at 50% confluency were infected with rADF-4-ΔC or rADF-4 containing recombinant viruses at MOI=10. Three days postinfection cells were fixed with methanol at −20 °C. Cover slips were incubated with mouse anti-His_6 or rat anti-HA monoclonal antibodies (Roche) at a 1:300 dilution followed by Texas Red conjugated anti-mouse or Cy2 conjugated anti-rat secondary IgG at 1:500 dilution. Cells were observed with an Olympus BX51 fluorescence microscope, and images were taken with a Magnafire SP camera or analyzed by confocal microscopy.

Transmission Electron Microscopy. For ultrastructural studies, *rADF*-4 fiber or ΔC aggregates were adsorbed onto Formvar-coated grids, negatively stained with uranyl acetate, and viewed and photographed in TECNAI 12. Alternatively, the material was suspended in 3.5% low-melting agar. Agar samples were postfixed in a mixture of 0.1% osmium tetroxide and 1.5% potassium ferrocyanide, dehydrated in ascending concentrations of ethanol up to 100%, infiltrated, and embedded with resin (EM-BED-812, Electron Microscopy Sciences). Ultrathin sections were collected on grids and then contrasted with uranyl acetate and lead citrate before being subjected to microscopy.

Silk Degumming. *Bombyx mori* silk was degummed in an alkaline solution containing NaOH 0.05 g, $NaHCO_3$ 0.2 g, and sodium dodecyl sulfate (SDS) 0.03 g per 100 mL at 98 °C (boiling time: 70 min). Degummed silk was thoroughly rinsed with warm distilled water, paper filtered twice, vacuum-dried at room temperature, and then extracted with petroleum ether 40−60 °C to remove residual fatty acids. The fibers were vacuum-dried at room temperature before analysis.

Differential Scanning Calorimeter (DSC) Measurement. Thermal analysis was done on 0.5−3 mg fibroin samples using a Mettler DSC 822e thermoanalyzer and an aluminum sample pan under an inert nitrogen atmosphere. The thermograms ranged from 25 to 350 °C at 5 °C/min heating rate.

Results and Discussion

Previously, we have shown that out of the two partial dragline cDNA clones derived from *A. diadematus*, which contain an artificial N-terminus, part of the repetitive units, and the complete C-termini of the natural proteins (see Figure 1A), only the more hydrophobic, spidroin1-like rADF-4 protein undergoes self-assembly in live cells into fibers, which are similar in form, shape, and chemical characteristics to authentic fibers obtained from the animal.[18] As we can genetically manipulate the sequence of the recombinant baculovirus transfer vector used for expression at will, we produced a new *rADF*-4-ΔC, in which the entire C-terminal domain was deleted from the parental *rADF*-4 and a stop codon introduced directly after the repetitive coding part (Figure 1A and Materials and Methods section). A recombinant *rADF*-4-ΔC baculovirus was prepared and used to infect insect cells, the expression of which was detected by immunoblotting of infected cell lysates using antibodies for an N-terminal His_6-tag. A band close to that of the calculated 50 kDa could be detected at 52 kDa as compared to the higher 60 kDa parental rADF-4 band (Figure 1B). We then used light microscopy as well as immunofluorescence to observe the structures formed by the rADF-4-ΔC in the infected cells. While *rADF*-4 infected cells exhibited the typical fiber pattern, the truncated protein was found in multiple round rosette- or bagel-shaped aggregates, which were distributed homogeneously in the cytoplasm (Figure 1C). We then wondered whether the ΔC aggregates were chemically stable like the fibers and aggregates formed by rADF-4, and for this, we lysed the expressing cells with a 10% SDS solution that disrupts all protein assemblies and structures but for which we have shown that the rADF-4 fibers and complexes are resistant. Interestingly, the ΔC complexes were not affected by this treatment unlike the spidroin 2-like, rADF-3 aggregates,[18] which were totally disrupted under the same conditions (not shown). Thus, it seems that, although the deletion of the C-terminal domain abrogated the final fiber formation, it did not affect the basic assembly of protein typical to rADF-4. This is in accord with recent reports that repetitive domain polypeptides can aggregate without the presence of the C-termini, which do however enhance this aggregation.[17]

Next, we asked what would happen when the two *ADF*-4 forms are coexpressed: Will the two types of structures arise independently? Will only one of them prevail, or perhaps none will be formed and a new structure will arise? To answer this, we first had to be able to distinguish between the two forms of the protein when coexpressed, and thus, we constructed another *rADF*-4 virus in which the His_6-tag was replaced with an HA-tag. After verifying that expression using the HA-tagged *rADF*-4 virus does indeed give rise to fibers that are specifically stained with anti-HA antibodies (Figure 2A), we assayed the expression

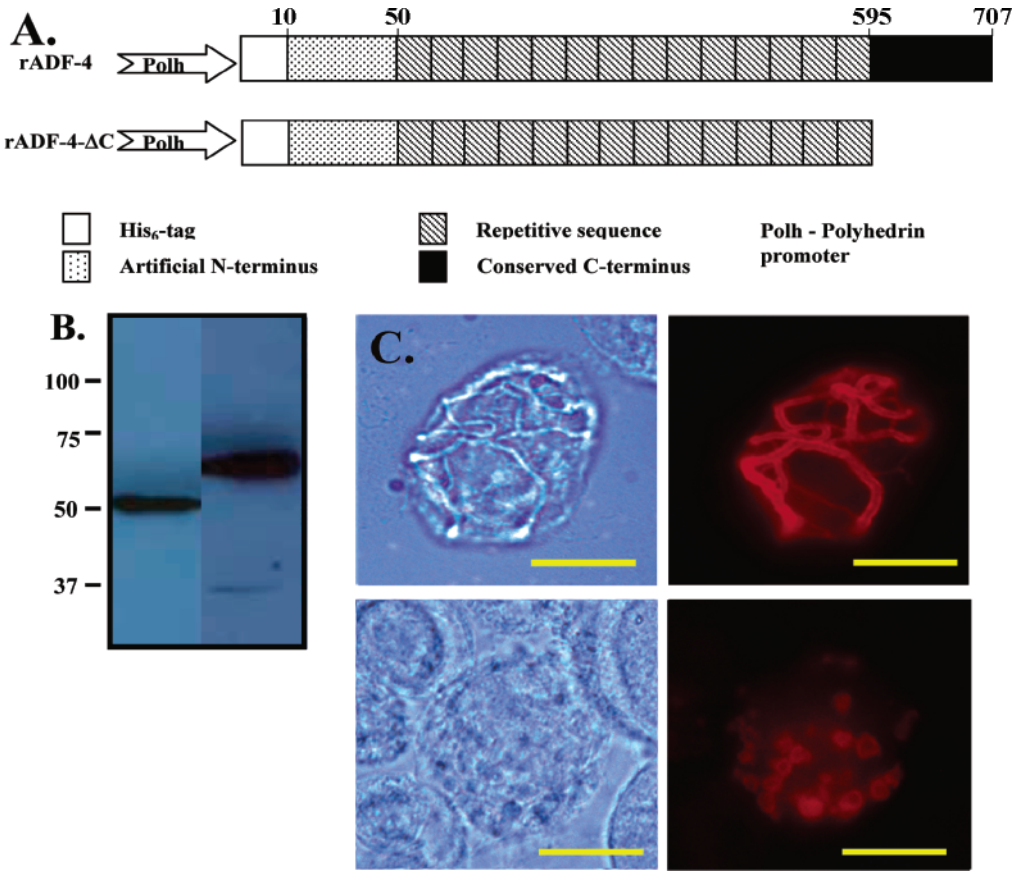

Figure 1. Expression of *rADF*-4 and *rADF*-4-ΔC in Sf9 cells. (A) Structure of the expression constructs used in this study. The numbers refer to the corresponding amino acids of the encoded proteins (B) Western-blot of *Sf9* cells expressing *rADF*4-ΔC (left lane) and *rADF*-4 (right lane). Cell lysates were separated on SDS-PAGE, blotted, and probed with anti-His_6-tag antibodies. The sizes in kilodalton are indicated on left. (C) Filament in *rADF*-4-expressing cell, as seen with light microscopy (upper left panel) or with regular fluorescence microscopy using anti-His_6-tag antibodies (upper right panel) and aggregates in *rADF*-4-ΔC expressing cell, as seen with light microscopy (lower left panel) or with regular fluorescence microscopy (lower right panel). The scale bars represent 10 μm.

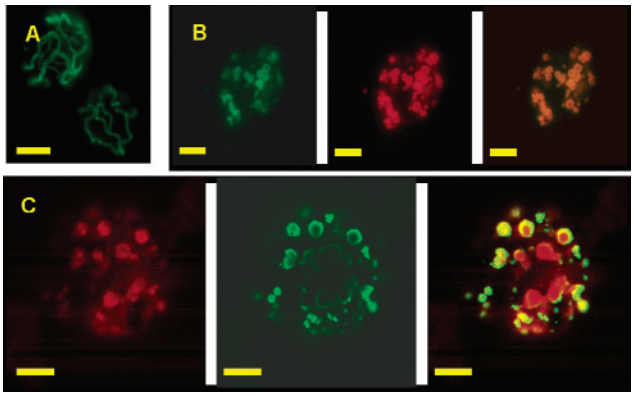

Figure 2. Immuno-staining of HA-tagged rADF-4 and His_6-tagged rADF-4-ΔC in *Sf9* cells. (A) Fibers in *rADF*4-expressing cells, as seen with regular fluorescence microscopy. (B) Aggregates in a cell coinfected with *rADF*4 and *rADF*4-ΔC viruses stained with anti-HA tag (left panel) and anti-His_6 tag (middle panel). Colocalization of both proteins is shown in the right panel. (C) Confocal microscopy of a coinfected cell, which was double-stained as above, demonstrating the rADF-4-ΔC (left) and rADF-4 (middle) nature of the formed aggregates. A Merge image (right) revealing the substructure of the aggregates: While rADF-4-ΔC (red) composes the core, rADF-4 (green) is located at the peripheral zone of the aggregates. The scale bars represent 5 μm.

of each protein in insect cells infected with both the *rADF*-4 and *rADF*4-ΔC viruses. Intriguingly, in a large majority of the cells that expressed both proteins, the staining was similar to that of cells expressing ΔC only (Figure 2B). Thus, out of all the possible outcomes of the coexpression, the predominance of one form, namely, that of ΔC occurred, indicating that the presence of the truncated form interrupted with the formation of the normal rADF-4 fibers. What is the organization of the two forms in the ΔC-like structures upon coexpression?

For this, we used confocal microscopy, which demonstrated that the two forms in the aggregates were not randomly distributed but rather formed a "stuffed cookie" arrangement with the inner part or "filling" staining for the ΔC (Figure 2C, left), while the outer part or "coating" staining for HA-rADF-4 (Figure 2C, middle), a pattern verified by the merged images of the two stainings (Figure 2C, right).

Thus, it seems that the two forms tend to segregate and create homogeneous structures; however, they do have the ability to interact via their repetitive regions leading to the coating of the ΔC by rADF-4, which seems to abrogate fiber formation from the latter. It is possible that the ΔC "bagel" aggregates form as a result of a faster assembly kinetics, as no oriented assembly takes place, and then, these aggregates serve as a scaffold or mold for the rADF-4 envelope.

To gain more insight into the different macromolecular behavior of the different proteins, we turned to ultrastructural analysis using TEM, in which we inspected the different rADF-4 structures at higher magnifications. As can be seen in Figure 3A in a view of purified fibers mounted on top of EM grids, the rADF-4 fibers showed discrete and ordered fiber shapes that are composed of aligned long nanofibrils packed very closely together, while in the ΔC case (Figure 3B), the aforementioned

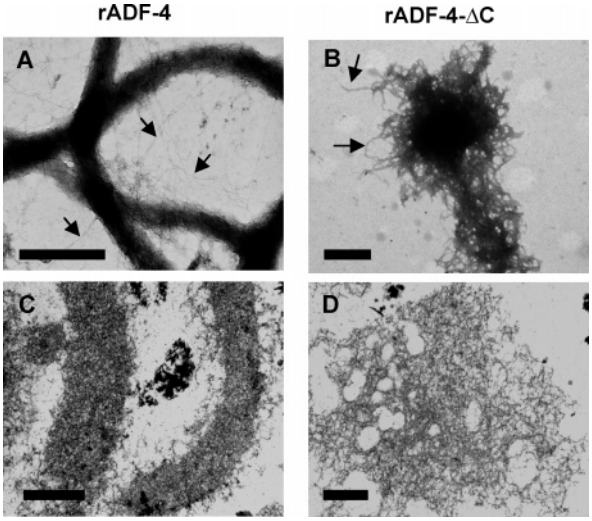

Figure 3. Electron microscope analysis of rADF-4 fibers and rADF4-ΔC complexes. Purified fibers from *rADF*-4 (A,C) or complexes from *rADF*-4-ΔC expressing cells (B,D) were either directly subjected to TEM (A,B) or were first embedded in agar and sectioned prior to TEM (C,D). Note the difference in the size and shape of the nanofibers between A and B (arrows). The scale bars represent 0.5 μm.

round aggregates are present with numerous fibrils protruding from them. Thus, the ΔC structures are also composed of nanofibers, which associate to constitute the final larger "bagel" structures, albeit the ΔC nanofibrils are different from those of rADF-4: the former are about 20 nm in diameter as compared to about 5 nm in diameter for the later. This change in width has also been reported in the recent report where peptides with or without the C-terminus were compared.[17] When sections of agar-embedded fibers/aggregates were analyzed by TEM, we again saw the difference in the density of material packing between the two forms. The rADF-4 sections (Figure 3C) displayed the tight shape of an oriented fiber, while the ΔC aggregates are more loosely arranged nonoriented material (Figure 3D). Thus, here we see a prominent difference from the prior study,[17] as we observe a change in the consistency and form of the basic nanofibers as well as in their length. The difference may well be due to the very different experimental systems used and is also likely due to the nature of monomers employed, since we have used a 60 kDa protein (rADF-4) as compared to the smaller, around 20 kDa polypeptides in the former study. This difference in size changes the ratio between the C-terminal to repetitive part domains, which may change the steps in fiber formation, such as the size of initial micelles and the ensuing globule formation demonstrated in *Bombyx mori* silk and suggested also for spider fibers.[19]

We also expect that, had we been able to express the much larger full-length *ADF*-4 gene coding for an ~250 kDa protein, we would have received fibers that display different properties; although it may well be that these proteins, being of a very large MW, would be prone to enter a gel-like state in high concentrations[2,8,9] and would not form fibers in our system.

Next, we have employed physical analysis methods to study the properties of the r-ADF-4 fibers and compare them to those of the rADF4-ΔC form. As these fibers have never been subjected to physical or mechanical examination, it is important to use such methods in order to better understand their structure and properties in relation to natural dragline silk. For this purpose, we used the calorimetric assay differential scanning calorimetry (DSC) to study our insect cell-derived fibers. DSC measures changes in the heat content of a sample as the temperature is consistently elevated, which allows detection of changes in heat absorption or emission, reflecting major structural changes and phase transitions. When we subjected purified r-ADF-4 fibers to DSC, we detected two endothermic peaks, a minor peak at 140−142 °C with a maximum at 141 °C and a major peak at 208−247 °C with a maximum at about 230 °C (Figure 4). A thermal change close to the first peak at 141 °C was previously assigned to disruption of α-helical structures of regenerated *Bombyx mori* (silkworm) silk,[20] which were induced by HFIP, while in this case, it may represent disruption of β-turn spiral structures found in the glycine-rich parts of dragline silks such as ADF-4,[11,21] which are unlikely to contain α-helices.[1,2] The exact structural motif underlying this endotherm may be resolved by further analyses such as X-ray diffraction.

The large prominent peak at 230 °C most likely represents the disruption of the polyalanine β-sheet "crystalline" regions,

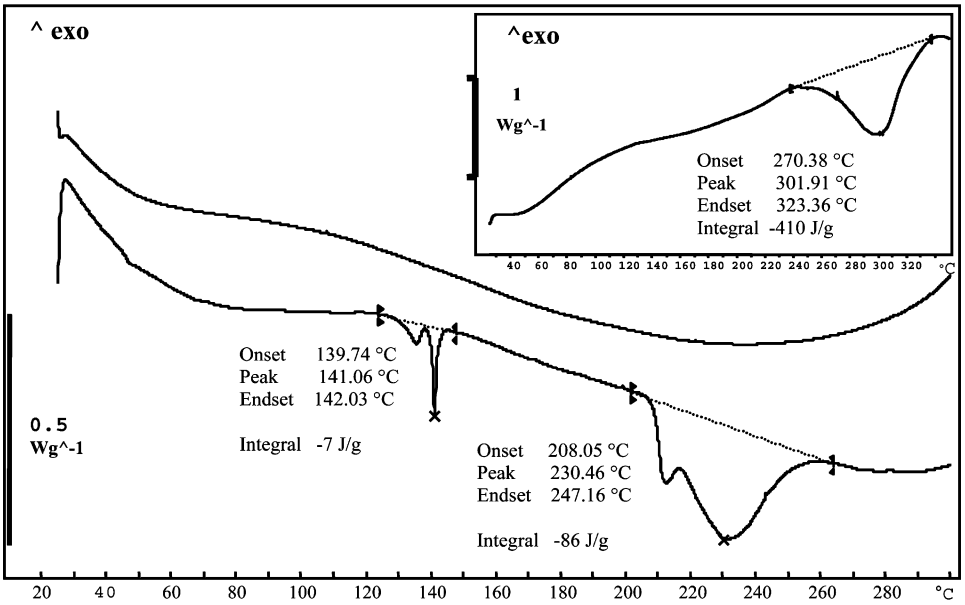

Figure 4. DSC curves of rADF-4 fibers, *Bombyx mori* silk, and rADF-4-ΔC aggregates. rADF-4 fibers display two endothermic peaks at 141 °C and at 230 °C (lower curve). *Bombyx mori* silk displays one endothermic peak at 301 °C (inset). rADF-4-ΔC aggregates display a smooth curve with no detectable peaks (upper curve).

which are typical to dragline fibers. Interestingly, a similar thermal decomposition point was reported for natural dragline fibers obtained from another spider species—*Nephila clavipes*.[22] To compare the thermal behavior of another β-sheet structure to ours, we turned to silk extracted from the silkworm *Bombyx mori*, which we subjected to DSC and found a large endotherm extending from 270 to 323 °C with a maximum at 301 °C (Figure 4, inset), corresponding to previous reports showing similar endotherms attributed to the decomposition of the β-sheet zones.[23−25] The *B. mori* heavy-chain fibroin contains large domains of polyglycylalanine (GA), which constitute 40−50% of its volume,[26] while spider dragline proteins contain much shorter polyalanine stretches, and their crystalline content is estimated to be from 10% to 25% of their volume.[1,10,27] It could then be expected that the *B. mori* fibroin endotherm would be larger than that of the r-ADF-4 dragline, and indeed, the integrated energy contents of the endotherms are 410 and 86 J/g, respectively. Since we presume that polyAG crystalline regions form more tightly packed β-sheet structures than the polyA regions of the dragline silks, due to the shorter predicted glycine−glycine intersheet distances,[1,28] the difference in the position of the *B. mori* silk and rADF-4 endotherms can also be understood. However, other explanations are also possible; for example, we can speculate that perhaps lower initiation energy is necessary to disrupt the smaller crystalline regions in the spider fibers, which could result in a lower decomposition point. Thus, the calorimetric evidence strongly suggests that the rADF-4 fibers demonstrate the structural attributes of natural dragline fibers. This result gives further credence to the use of recombinant fibers produced by the baculovirus system as a model for authentic dragline fibers.

Finally, we subjected purified rADF-4-ΔC material to DSC analysis and have obtained a smooth curve indicating a nonstructured "amorphous"-like material (Figure 4), very unlike the parental rADF-4. From this result, we can conclude that the absence of the C-terminal domain and consequently of ordered superfiber formation leads to the loss of the characteristic ordered structures of dragline silks, foremostly the typical β-sheet crystalline regions, which confer strength to the fiber. In light of these results, the typical crystalline regions and perhaps also structures in the glycine-rich repeats can only form when the C-terminal domain confers ordered assembly of the final superfibers.

In conclusion, we have shown that the C-terminal part of the dragline spider silk has an important role in formation of the dragline-like fiber in our system. This indicates that the high conservation of this domain between draglines is due to its function in fiber assembly, which was thought to be mostly orchestrated by the prominent major repetitive domain of these proteins. It is interesting that, while a basic rudimentary fibril structure can be formed without the C-terminal domain, the final organization into the macromolecular fiber structure is dependent on this domain that is essential for the correct fiber density and orientation. By the use of thermal analysis, we demonstrated that the rADF-4 fibers are structurally ordered, exhibiting a prominent phase transition, which can be attributed to the disruption of the crystalline β-sheet structures typical to dragline silks and that the deletion of the C-terminus led formation of stable aggregates of fibrils, which however showed no prominent macromolecular structures. Further, as rADF-4 fibers efficiently assemble in the cytoplasm of the host insect cells and since disulfide bonds are not supposed to occur in the cytoplasm of cells but rather in the secretory compartment, the critical role we have demonstrated here for the C-terminal domains in fiber orientation does not depend on covalent bond formation. This said, our system and the natural one are different, and thus, such bonds could still be important for dragline fiber formation and may also affect its mechanical properties in the natural spinning process. Future structural analyses and models of spider silk formation should take into account that the C-terminal domain is essential for the ordered assembly of these fibers in this cell-based system, which may be most relevant to the native formation of spider threads.

Acknowledgment. We wish to thank Dr. Tsafi Danieli for help and advice with insect cells and baculovirus work. We also express our gratitude to Dr. Naomi Melamed-Book for confocal analysis and Dr. Steve Darren for advice on thermal analysis. Further thanks to Yael and Iddo Gat for supplying us with hatched silkworm cocoons.

Abbreviations

rADF, recombinant *Araneus diadematus* fibroin
MaSp, major ampullate gland spidroin
Sf, *Spodoptera frugiperda*
HA, influenza hemaglutinin
ORF, open reading frame
MOI, multiplicity of infection
TEM, transmission electron microscopy
HFIP, hexafluoro-2-propanol.

References and Notes

(1) Craig, C. L. *Spiderwebs and silk*; Oxford University Press: Oxford, 2003.
(2) Vollrath, F.; Knight, D. P. *Nature (London)* **2001**, *410*, 541−548.
(3) Winkler, S.; Kaplan, D. L. *J. Biotechnol.* **2000**, *74*, 85−93.
(4) Hinman, M. B.; Lewis, R. V. *J. Biol. Chem.* **1992**, *267*, 19320−19324.
(5) Guerette, P. A.; Ginzinger, D. G.; Weber, B. H.; Gosline, J. M. *Science* **1996**, *272*, 112−115.
(6) Vollrath, F. *Int. J. Biol. Macromol.* **1999**, *24*, 81−88.
(7) Rising, A.; Nimmervoll, H.; Grip, S.; Fernandez-Arias, A.; Storckenfeldt, E.; Knight, D. P.; Vollrath, F.; Engstrom, W. *Zool. Sci.* **2005**, *22*, 273−281.
(8) Candelas, G.; Candelas, T.; Ortiz, A.; Rodriguez, O. *Biochem. Biophys. Res. Commun.* **1983**, *116*, 1033−1038.
(9) Xu, M.; Lewis, R. V. *Proc. Natl. Acad. Sci. U.S.A.* **1990**, *87*, 7120−7124.
(10) Gosline, J. M.; Guerette, P. A.; Ortlepp, C. S.; Savage, K. N. *J. Exp. Biol.* **1999**, *202 Pt 23*, 3295−3303.
(11) Hinman, M. B.; Jones, J. A.; Lewis, R. V. *Trends Biotechnol.* **2000**, *18*, 374−379.
(12) Hayashi, C. Y.; Shipley, N. H.; Lewis, R. V. *Int. J. Biol. Macromol.* **1999**, *24*, 271−275.
(13) Bini, E.; Knight, D. P.; Kaplan, D. L. *J. Mol. Biol.* **2004**, *335*, 27−40.
(14) Motriuk-Smith, D.; Smith, A.; Hayashi, C. Y.; Lewis, R. V. *Biomacromolecules* **2005**, *6*, 3152−3159.
(15) Beckwitt, R.; Arcidiacono, S. *J. Biol. Chem.* **1994**, *269*, 6661−6663.
(16) Sponner, A.; Unger, E.; Grosse, F.; Weisshart, K. *Biomacromolecules* **2004**, *5*, 840−845.
(17) Sponner, A.; Vater, W.; Rommerskirch, W.; Vollrath, F.; Unger, E.; Grosse, F.; Weisshart, K. *Biochem. Biophys. Res. Commun.* **2005**, *338*, 897−902.
(18) Huemmerich, D.; Scheibel, T.; Vollrath, F.; Cohen, S.; Gat, U.; Ittah, S. *Curr. Biol.* **2004**, *14*, 2070−2074.
(19) Jin, H. J.; Kaplan, D. L. *Nature (London)* **2003**, *424*, 1057−1061.
(20) Drummy, L. F.; Phillips, D. M.; Stone, M. O.; Farmer, B. L.; Naik, R. R. *Biomacromolecules* **2005**, *6*, 3328−3333.
(21) van Beek, J. D.; Hess, S.; Vollrath, F.; Meier, B. H. *Proc. Natl. Acad. Sci. U.S.A.* **2002**, *99*, 10266−10271.
(22) Cunniff, P. M.; Fossey, S. A.; Auerbach, M. A.; Song, J. W.; Kaplan, D. L.; Wade Adams, W.; Eby, R. K.; Mahoney, D.; Vezie, D. L. *Polym. Adv. Technol.* **1994**, *5*, 401−410.
(23) Freddi, G.; Pessina, G.; Tsukada, M. *Int. J. Biol. Macromol.* **1999**, *24*, 251−263.

(24) Zhao, C.; Yao, J.; Masuda, H.; Kishore, R.; Asakura, T. *Biopolymers* **2003**, *69*, 253−259.
(25) Marsano, E.; Corsini, P.; Arosio, C.; Boschi, A.; Mormino, M.; Freddi, G. *Int. J. Biol. Macromol.* **2005**, *37*, 179−188.
(26) Craig, C. L.; Riekel, C. *Comp. Biochem. Physiol., B* **2002**, *133*, 493−507.
(27) Simmons, A. H.; Michal, C. A.; Jelinski, L. W. *Science* **1996**, *271*, 84−87.
(28) Warwicker, J. O. *J. Mol. Biol.* **1960**, *2*, 350−362.

BM060120K